Improving Performance of GNSS Acquisition Systems by Optimizing TM-CFAR Thresholds Using Metaheuristics

Elbahdja Ourfella, Sabra Benkrinah, and Naceur Aounallah

Kasdi Merbah University, Ouargla, Algeria

https://doi.org/10.26636/jtit.2026.2.2518

Abstract — Signal acquisition is one of the key signal processing tasks performed by global navigation satellite system (GNSS) receivers. It involves detecting the presence or absence of a signal by comparing it with a predefined threshold, which can be either fixed or adaptive. This study focuses on optimizing the threshold of the trimmed mean constant false alarm rate (TM-CFAR) detector under Rayleigh fading conditions, employing metaheuristic optimization techniques, due to their proven efficacy in solving complex optimization problems. Furthermore, two TM-CFAR detectors are applied to the data and pilot channels of the GNSS system. Their outputs are then combined using two logical fusion strategies: AND and OR rules. Simulation results demonstrate that the optimized thresholds improve the performance of the GNSS signal acquisition system.

Keywords — GNSS, metaheuristic optimization techniques, Rayleigh fading channel, signal acquisition, TM-CFAR detector

1. Introduction

Global navigation satellite systems (GNSS) include satellite constellations such as GPS, Galileo, Glonass or BeiDou, developed to deliver precise positioning and timing information to users worldwide [1], [2]. Among these, the Global Positioning System (GPS) is the earliest and remains the only fully operational system enjoying widespread adoption. It comprises a constellation of 32 satellites designed to provide continuous service regardless of weather conditions, with growing global demand [3]. However, as shown in Fig. 1, GNSS signals, particularly those from GPS, are susceptible to significant degradation due to power attenuation and multipath fading, especially under challenging visibility or environmental conditions.

GNSS signals typically comprise two distinct components: data and pilot channels. The data channel transmits the navigation message, whereas the pilot channel, carrying a minimum amount of or no data at all, is primarily utilized for precise pseudorange estimates. Signal acquisition is a fundamental process in ensuring the accuracy and reliability of GNSS-based positioning. Advancements in signal processing algorithms and optimization methodologies continue to enhance the performance of GNSS receivers, particularly in challenging signal environments.

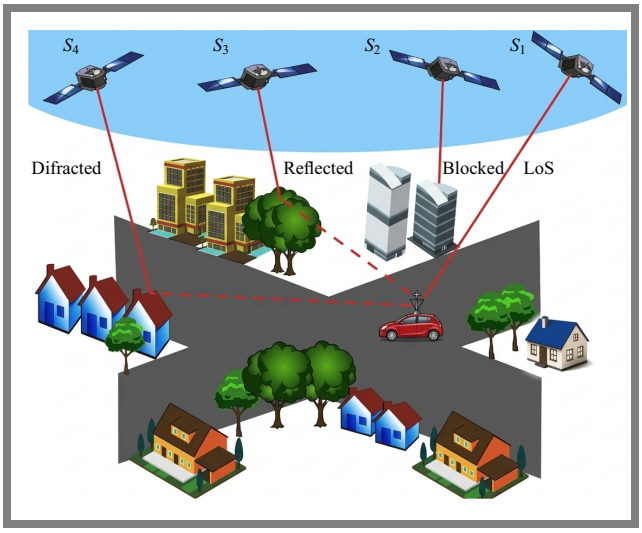

Fig. 1. GPS signal fading model.

In this context, the authors of [1] introduced an adaptive thresholding approach based on the cell-averaging constant false alarm rate (CA-CFAR) technique for the altBOC E5 signal under both Rayleigh and Gaussian fading conditions. Their findings indicated promising detection performance. In [2], an analytical formulation for the detection and false alarm probabilities in collective detection scenarios employing the CA-CFAR detector is proposed. To determine the optimal thresholds for CA-CFAR detectors, metaheuristic optimization techniques are applied in [4], in the context of Rayleigh fading channels. Four advanced metaheuristic algorithms, namely particle swarm optimization (PSO), biogeography-based optimization (BBO), firefly algorithm (FA), and simulated annealing (SA), are implemented and compared.

In satellite communication systems, multipath fading and interference make the signal environment non-homogeneous, reducing the effectiveness of the CA-CFAR detector. The TM-CFAR detector improves performance by ignoring the strongest and weakest signals in the reference window, thus helping to reduce the impact of random changes. This results

in a more precise detection threshold and a more stable false alarm rate. Therefore, TM-CFAR is more reliable than CA-CFAR in environments with interference and multipath effects [5].

This study explores the integration of the TM-CFAR detector which replaces its CA-CFAR counterpart during the acquisition phase of a GNSS receiver. By leveraging the enhanced robustness of TM-CFAR in non-homogeneous environments, the proposed approach aims to improve signal detection under challenging conditions. To optimize the detector's performance, metaheuristic optimization techniques are employed. This combination is expected to enhance the overall efficiency and reliability of the GNSS data acquisition process.

To achieve this objective, four different metaheuristic optimization algorithms are employed, and their performance is evaluated and compared in order to identify the most effective optimization strategy for enhancing the outcomes achieved with the use of the TM-CFAR detector. These include the following: particle swarm optimization (PSO), whale optimization algorithm (WOA), ant lion optimizer (ALO), and grey wolf optimizer (GWO).

The remainder of this paper is organized as follows. In Section 2, the proposed adaptive acquisition system operating in a Rayleigh-fading channel with the use of the TM-CFAR processor is presented. In Section 3, the system is analyzed and expressions for the detection and false-alarm probabilities as functions of the TM-CFAR parameters are provided. In Section 4, various metaheuristic optimization techniques are reviewed. In Section 5, the acquisition and detection performance of the proposed scheme are evaluated based on simulation results. Finally, concluding remarks are discussed in Section 6.

2. System Description

This study focuses on the signal acquisition phase, which is a critical stage in the GNSS receivers – see Fig. 2. This phase not only detects the presence or absence of the desired signal but also estimates its key parameters, such as code delay and Doppler frequency. The acquisition process is typically formulated as a joint detection and estimation problem, highlighting its importance in achieving accurate and reliable signal processing in GNSS systems [6].

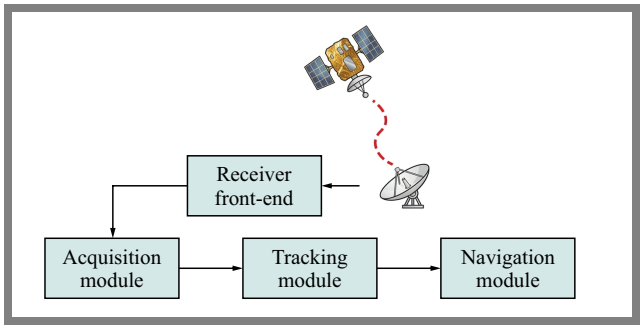

Fig. 2. GNSS receiver scheme.

The signal model under consideration comprises additive Gaussian noise, multiplicative noise, and the signal from the visible satellite. However, the analysis is simplified by assuming that multiplicative noise is sufficiently weak to be neglected, allowing the focus to remain on the effects of the additive noise and the satellite signal in the acquisition process [4], and it is described as follows:

$$r(t) = \sqrt{2C}\, c(t-\tau)\, \cos\left(2\pi F_D\, t + \phi\right) + n(t)\,, \qquad (1)$$

where C and $c(t)$ are the signal power and the spreading code, respectively. τ and F_D are the code delay and the Doppler frequency, respectively. ϕ is a uniformly distributed random phase in the interval $[0, 2\pi]$. Finally, $n(t)$ is the additive noise.

The signal described in Eq. (1) is initially multiplied by a locally generated carrier and spreading code. The resulting signal is then processed through incoherent integration to accumulate energy over time. Subsequently, the squared magnitude of the integrated output is computed to form the decision statistic.

The diagram of the proposed acquisition system is depicted in Fig. 3.

3. System Analysis

3.1. TM-CFAR Processor

In the presence of urban interference and multipath conditions, as well as to enhance detection performance, a constant false alarm rate technique is introduced at the detection and decision level. This technique offers a significant advantage due to its ability to adapt to varying ambient noise levels, enabling the reliable identification of visible GNSS satellites. Although CFAR techniques are well established in radar applications, their use in GNSS systems remains relatively limited.

In this work, two TM-CFAR detectors are implemented at two stages: at the output of the pilot channel and at the output of the data channel of the GNSS receiver.

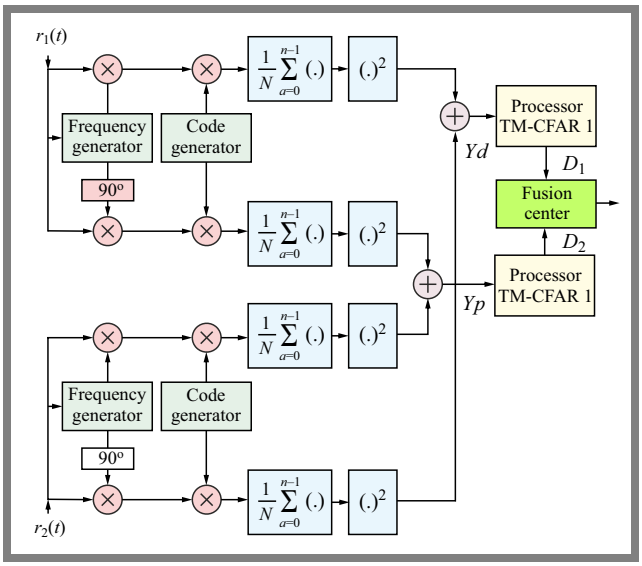

Fig. 3. Proposed adaptive acquisition system.

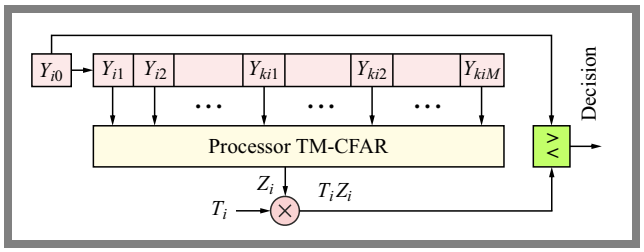

Fig. 4. Functional diagram of the TM-CFAR detector.

The functional diagram of the TM-CFAR detector, as shown in Fig. 4, consists of M cells that precede the cell under test (CUT). It comprises sorting, censoring and summation routines. First, the amplitudes of the samples, $Y_{i1}, Y_{i2}, \ldots, Y_{iM}, i = d, p$ for data and pilot channels, respectively, are ordered from the smallest value to the largest one as follows:

$$Y_{(i1)} \leqslant Y_{(i2)} \leqslant \cdots \leqslant Y_{(iM)} \, . \tag{2}$$

After censoring k_{i1} samples from the lower end and k_{i2} samples from the upper end of each detector, $i = d, p$, the noise power level Z_i is estimated by performing the arithmetic sum of the remaining reference cells content of each TM-CFAR detector [7]:

$$Z_i = \sum_{j=k_{i1}+1}^{M-k_{i2}} Y_{(ij)}, i = d, p \, . \tag{3}$$

With both detectors having the same number of reference cells M, the count of samples censored from the upper tail of each detector serves as an estimate of the number of samples containing multipath replicas.

Therefore, the values of k_{i1} and k_{i2}, $i = d, p$ are used to obtain the statistics Z_i $i = d, p$ and the scaling factors T_d and T_p that achieve the desired false alarm probabilities, P_{FA_i}, $i = d, p$ of the two adaptive detectors and, consequently, the overall desired false alarm rate P_{FA}.

Each factor T_i $i = d, p$ is determined according to the desired false alarm rate of the corresponding TM-CFAR detector. It is then multiplied by variable Z_i to obtain the adaptive threshold of each adaptive detector T_i Z_i.

3.2. Problem Definition and Formulation

In this section, we analyze the statistical detection process of the TM-CFAR detector in a GNSS acquisition system. To formulate the detection problem, we consider two cases:

- H_0 – the received signal contains only noise (signal absent),
- H_1 – the received signal contains the GNSS signal in addition to noise (signal present).

The probability density function (PDF) under the hypothesis H_1, $f_{Y_i/H_1}(y_i/H_1), i = d, p$, can be expressed as:

$$f_{Yi/H1}\left(y_i/H_1\right) = \frac{1}{1+\mu} \, e^{-\frac{y_i}{1+\mu}}, i = d, p, \; y_i \geqslant 0 \, , \tag{4}$$

where μ denotes the average signal-to-noise ratio (SNR) and y_i denotes the i-th received sample from either the pilot or data channel under hypothesis H_1. The PDF under hypothesis H_0 is given by:

$$f_{Yi/H_0}\left(y_i/H_0\right) = e^{y_i}, i = d, p, \; y_i \geqslant 0 \, . \tag{5}$$

In this situation, the false alarm probabilities P_{FAd} and P_{FAp} of the data and pilot channels can be calculated using the following expressions:

$$P_{FAd} = \prod_{i=1}^{M-k_{d1}-k_{d2}} Mv_i(T_d) \, , \tag{6}$$

$$P_{FAp} = \prod_{i=1}^{M-k_{p1}-k_{p2}} Mv_i(T_p) \, , \tag{7}$$

where

$$\begin{aligned} Mv_1(T_d) =& \frac{M!}{k_{d1}(M-k_{d1}-1)!(M-k_{d1}-k_{d2})} \\ & \times \sum_{i=0}^{k_{d1}} \frac{\binom{k_{d1}}{j}(-1)^{k_{d1}-i}}{\frac{M-i}{M-k_{d1}-k_{d2}}+T_d} \end{aligned} \, , \tag{8}$$

$$\begin{aligned} Mv_1(T_p) =& \frac{M!}{k_{p1}(M-k_{p1}-1)!(M-k_{p1}-k_{p2})} \\ & \times \sum_{i=0}^{k_{p1}} \frac{\binom{k_{p1}}{j}(-1)^{k_{p1}-i}}{\frac{M-i}{M-k_{p1}-k_{p2}}+T_p} \end{aligned} \, , \tag{9}$$

$$Mv_i(T_d) = \frac{a_{id}}{a_{id}+1}, \;\; id = 2, \ldots, M-k_{d1}-k_{d2} \, , \tag{10}$$

and

$$Mv_i(T_p) = \frac{a_{ip}}{a_{ip}+1}, \;\; ip = 2, \ldots, M-k_{p1}-k_{p2} \, , \tag{11}$$

with

$$a_{id} = \frac{M-k_{d1}-id+1}{M-k_{d1}-k_{d2}-i+1} \, , \tag{12}$$

and

$$a_{ip} = \frac{M-k_{p1}-ip+1}{M-k_{p1}-k_{p2}-i+1} \, . \tag{13}$$

The detection probabilities P_{Dd} and P_{Dp} of the data and pilot channels are obtained by replacing T_d and T_p with $T_d/(1+\mu)$ and $T_p/(1+\mu)$, in Eqs. (6) and (7), respectively.

The introduction of a fusion center, comprising two TM-CFAR detectors, aims to enhance the detection performance in any communication system. The fusion center will combine the results of the two TM-CFAR detectors, resulting in an increased probability of detection while maintaining a desired probability of false alarm. Two fusion methods are implemented in this present work: the AND rule and the OR rule [4].

For the "AND fusion rule", the global detection and false alarm probabilities are given by:

$$P_D = P_{Dd} \times P_{Dp} \, , \tag{14}$$

$$P_{FA} = P_{FAd} \times P_{FAp} \, . \tag{15}$$

For the "OR fusion rule", the global detection and false alarm probabilities are as follows:

$$P_D = 1 - \left[(1-P_{Dd}) \times (1-P_{Dp})\right] \, , \tag{16}$$

$$P_{FA} = 1 - \left[(1-P_{FAd}) \times (1-P_{FAp})\right] \, . \tag{17}$$

The optimization problem under consideration involves identifying a set of six unknown parameters: T_p, T_d, k_{p1}, k_{p2}, k_{d1}, and k_{d2} that significantly impact the performance of the system. Determining their optimal values is crucial to ensuring the desired system's behavior and maximizing its overall performance.

The objective function governing this optimization problem can be expressed as:

$$f(T_p, T_d, k_{d1}, k_{d2}, k_{p1}, k_{p2}) = \left|1 - P_D\right| + \left(\frac{1}{P_{FA0}} \times \left|P_{FA} - P_{FA0}\right|\right), \quad (18)$$

where P_{FA0} is the desired false alarm rate, and symbol $|\,.\,|$ gives the absolute value.

The goal is to minimize f by appropriately tuning the six unknown parameters. Classical optimization methods often exhibit limitations when addressing complex, non-linear, non-differentiable, or high-dimensional objective functions. In such cases, metaheuristic algorithms provide an effective alternative by offering flexible and computationally efficient mechanisms for global search and convergence.

3.3. Problem Solving Methodology

To solve the present optimization problem, several metaheuristic techniques are employed, including PSO, WOA, ALO and GWO. These population-based algorithms are capable of efficiently exploring the solution space and converging toward near-optimal solutions without requiring explicit gradient information or closed-form expressions of the objective function.

By applying these algorithms, the optimal values of T_p, T_d, k_{p1}, k_{p2}, k_{d1}, and k_{d2} can be effectively determined, thereby minimizing the objective function f and achieving the desired trade-off between detection performance and false alarm rate P_{FA}.

4. Optimization Techniques

4.1. Particle Swarm Optimization

PSO stands as a widely recognized stochastic swarm-based algorithm inspired by nature [8], [9]. The algorithm has attracted numerous researchers over the past decade due to its simplicity. The concept and formulation of the PSO algorithm were inspired by observations of the social behavior of bird flocks and fish schools [10].

In PSO, a group of particles (like a flock of birds) explores the problem space. Each particle shares its best position and fitness with others in the swarm, adding some randomness to decide its next move. This movement is influenced by each particle's past and the overall swarm's direction. After all particles update their positions in one iteration, the process repeats, exploring areas near the current best solutions. Eventually, the swarm tends to converge to the optimum of the objective function.

The rate of convergence depends heavily on the PSO variant and the control parameters. Particle speed and position updates follow the rules outlined in [8]:

$$V_{id}^{k+1} = \omega V_{id}^{k} + c_1 r_1^k (P_{best_{id}}^k - x_{id}^k) + c_2 r_2^k (G_{best_{id}}^k - x_{id}^k) \quad (19)$$

and

$$x_{id}^{k+1} = x_{id}^k + V_{id}^{k+1}, \quad (20)$$

where V_{id}^k and x_{id}^k represent the speed and the position of the i particle in d dimension at k time, $P_{best_{id}}^k$ is the best position visited so far by the i-th particle, and $G_{best_{id}}^k$ is the best position visited so far by any particle in the swarm, c_1 and c_2 are the cognitive and social acceleration coefficients, while r_1 and r_2 are two diagonal matrices of random values generated within the [0, 1] interval.

4.2. Grey Wolf Optimization

GWO stems from the social leadership and hunting technique of gray wolves. The algorithm incorporates a mathematical representation of the wolf pack hierarchy inspired by their social hunting behavior, observed in gray wolves in nature.

In this algorithm, the population is divided into four groups:

- alpha (α) – the leader of the pack, responsible for decision-making (e.g., hunting strategies). It represents the best solution in the optimization process.
- beta (β) – subordinate wolves that assist α in decision-making. They represent the second-best solution.
- delta (δ) – wolves that follow α and β, helping to control the pack. These represent the third-best solutions.
- omega (ω) – the lowest-ranking wolves that follow the other wolves. These represent the rest of the population.

The three strongest wolves α, β, and δ, are considered to guide the other wolves ω toward promising areas in the search space. The best solution is denoted as the α wolf, followed by β and δ wolves, while the remaining solutions are classified as ω wolves. The optimization process in GWO is guided by α, β, and δ, which lead the ω wolves toward the global optimum [9]. The hunting process starts with wolves encircling their prey. This process can be expressed as follows:

$$\vec{D} = \left|\vec{C} \cdot \vec{X}_{prey}(t) - \vec{X}(t)\right|, \quad (21)$$

$$\vec{X}(t+1) = \vec{X}_{prey}(t) - \vec{A} \cdot \vec{D}, \quad (22)$$

where $\vec{X}(t)$ denotes the current position of a wolf, $\vec{X}_{prey}(t)$ represents the position of the prey (best-known solution), and vector $\vec{D}$ represents the distance between the position of a wolf and the prey, weighted by a random coefficient $\vec{C}$.
$\vec{A}$ and $\vec{C}$ are defined as follows:

$$\vec{A} = 2\,\vec{a} \cdot \vec{r_1} - \vec{a}, \quad (23)$$

$$\vec{C} = 2 \cdot \vec{r_2}, \quad (24)$$

where $\vec{r_1}$ and $\vec{r_2}$ are random vectors in the range [0, 1], while $\vec{a}$ decreases linearly from 2 to 0 over the course of iterations, controlling the balance between exploration (searching new areas) and exploitation (refining known solutions).

To simulate the cooperative guidance of α, β, and δ wolves, each wolf updates its position according to the influence of these three leaders:

$$\begin{aligned}\vec{D}_\alpha &= \left|\vec{C}_1 \cdot \vec{X}_\alpha - \vec{X}\right|,\\ \vec{D}_\beta &= \left|\vec{C}_2 \cdot \vec{X}_\beta - \vec{X}\right|,\\ \vec{D}_\delta &= \left|\vec{C}_3 \cdot \vec{X}_\delta - \vec{X}\right|.\end{aligned} \tag{25}$$

The final position of each wolf is then calculated as the mean of these three influences:

$$\vec{X}(t+1) = \frac{\vec{X}_1 + \vec{X}_2 + \vec{X}_3}{3}\,. \tag{26}$$

This mechanism allows the population to converge on its prey (the optimal solution) while maintaining a good balance between exploration and exploitation. The fitness function measures the quality of each candidate solution based on the defined optimization goal.

The main steps of the GWO algorithm are described as follows:

1) Initialize the population of gray wolves randomly within the search space.
2) Evaluate the fitness of each wolf.
3) Identify α, β, and δ wolves based on their fitness values.
4) The positions of the wolves are updated in accordance with Eqs. (21) – (25).
5) Reduce parameter $\vec{a}$ linearly to shift from exploration to exploitation.
6) Repeat the process until the termination criterion (maximum iterations or convergence) is met.

The α wolf represents the algorithm's best solution upon completion of the optimization.

4.3. Ant Lion Optimizer

The ALO is a swarm intelligence-based metaheuristic algorithm. It models the interaction between ants and antlions in nature [10].

The algorithm is inspired by the hunting behavior of antlions, which trap prey in the pits they dig. In our study, this behavior is modeled to guide the optimization of TM-CFAR detection thresholds in the GNSS acquisition system. The algorithm adaptively explores the solution space and exploits promising regions to improve detection performance, avoid local optima, and ensure a reliable convergence toward optimal threshold values. The algorithmic process comprises five steps: starting with the random walk process of ants, followed by trap construction, then ant trapping in the traps created by antlions, ant capture, and finally reconstruction of traps.

The antlion life cycle consists of two stages: larvae and adults. The first method of ant capture involves moving ant larvae in a circular path to dig a cone-shaped pit in the sand. Then, antlions use their massive jaws to throw sand out of the cone. They then wait for insects to be trapped at the bottom of the cone. Once captured, the prey is drawn towards the cone and consumed by the antlions. Finally, the remains of the ants are discarded outside the conical pit, and the pit is improved for the next prey to be hunted [11].

4.4. Whale Optimization Algorithm

Inspired by the natural hunting behavior of humpback whales, WOA algorithm mimics the way these whales hunt by targeting groups of krill or small fish on the water's surface. They form spiral bubble nets to encircle and capture their prey while diving and ascending toward the surface. This behavior is modeled in WOA through three strategies: prey encircling, prey searching (exploration phase), and spiral bubble-net attacking (exploitation phase).

The position of the i-th whale at iteration t is given by:

$$X_i^t = (x_{i,1}^t, x_{i,2}^t, \ldots, x_{i,D}^t),\;\; i = 1, 2, \ldots, N\,, \tag{27}$$

where N and D represent the whale population size and the dimensionality of the problem, respectively.

The mathematical formulation of the WOA strategies is provided in [13].

5. Performance Evaluation

For the simulation outcomes, the detection probability has been calculated using the Monte Carlo simulation method. It is provided by the following equation:

$$P_D = \frac{\text{Number of detections}}{\text{Number of all tested signal cells}}\,. \tag{28}$$

The results obtained assume that the environment is a Rayleigh fading channel. Table 1 summarizes the parameter values used to obtain these results.

Firstly, search intervals are defined on T_p, $T_d \in [0, 5]$, k_{d1}, k_{d2}, k_{p1} and $k_{p2} \in [1, \frac{M}{2}]$, where M denotes the reference window size of each detector. The initial population consists of 30 particles, for the AND and OR fusion rules.

The results present four detector cases: identical, different, symmetric, and asymmetric, comparing fixed-threshold and TM-CFAR detectors. In addition, four optimization methods were selected to calculate the unknown parameters of the two TM-CFAR detectors (WOA, ALO, GWO, and PSO). The effects of the number of reference cells, SNR variations, and the desired P_{FA} on the performance of the system are then investigated. Considering a signal-to-noise ratio of 60 dB-Hz, the results are summarized in four tables with the corresponding detection probabilities. These tables clearly demonstrate

Tab. 1. Simulation parameters used to obtain the desired results.

Parameter	Value
Sampling frequency fs	40.92 MHz
P_{FA}	10^{-4}
Number of iterations	100 000
Population size	500
Number of interferers O	3, 6

Tab. 2. Parameters estimated using the four optimization algorithms based on the number of cells with the AND fusion rule.

Number of cells	PSO	GWO	ALO	WOA
$M = 8$	$T = 1.7023$	$T = 3.5138$	$T = 1.5288$	$T = 1.7647$
	$k_1 = 1$	$k_1 = 2$	$k_1 = 1$	$k_1 = 4$
	$k_2 = 2$	$k_2 = 3$	$k_2 = 2$	$k_2 = 1$
	$P_D = 0.9770$	$P_D = 0.9731$	$P_D = 0.9793$	$P_D = 0.9735$
	$T = 0.5522$	$T = 1.5391$	$T = 0.8132$	$T = 0.6057$
$M = 16$	$k_1 = 5$	$k_1 = 6$	$k_1 = 5$	$k_1 = 5$
	$k_2 = 4$	$k_2 = 6$	$k_2 = 4$	$k_2 = 4$
	$P_D = 0.9820$	$P_D = 0.9822$	$P_D = 0.9815$	$P_D = 0.9862$
	$T = 1.7034$	$T = 1$	$T = 0.651$	$T = 3.4978$
$M = 32$	$k_1 = 7$	$k_1 = 11$	$k_1 = 11$	$k_1 = 4$
	$k_2 = 13$	$k_2 = 13$	$k_2 = 13$	$k_2 = 16$
	$P_D = 0.9891$	$P_D = 0.9793$	$P_D = 0.9860$	$P_D = 0.9889$

Tab. 3. Parameters estimated using the four optimization algorithms based on P_{FA} with the AND fusion rule.

Probability of false alarm	PSO	GWO	ALO	WOA
$P_{FA} = 10^{-4}$	$T = 1.7034$	$T = 1.7393$	$T = 0.651$	$T = 3.4978$
	$k_1 = 7$	$k_1 = 7$	$k_1 = 11$	$k_1 = 4$
	$k_2 = 13$	$k_2 = 13$	$k_2 = 13$	$k_2 = 16$
	$P_D = 0.9891$	$P_D = 0.9793$	$P_D = 0.9860$	$P_D = 0.9889$
$P_{FA} = 10^{-6}$	$T = 4.1283$	$T = 1.7564$	$T = 0.5916$	$T = 0.5071$
	$k_1 = 10$	$k_1 = 9$	$k_1 = 2$	$k_1 = 3$
	$k_2 = 13$	$k_2 = 15$	$k_2 = 12$	$k_2 = 12$
	$P_D = 0.9850$	$P_D = 0.9700$	$P_D = 0.9803$	$P_D = 0.9833$
$P_{FA} = 10^{-8}$	$T = 0.7270$	$T = 1.9737$	$T = 1$	$T = 0.9914$
	$k_1 = 10$	$k_1 = 5$	$k_1 = 10$	$k_1 = 4$
	$k_2 = 8$	$k_2 = 14$	$k_2 = 8$	$k_2 = 9$
	$P_D = 0.9676$	$P_D = 0.9524$	$P_D = 0.9558$	$P_D = 0.9552$

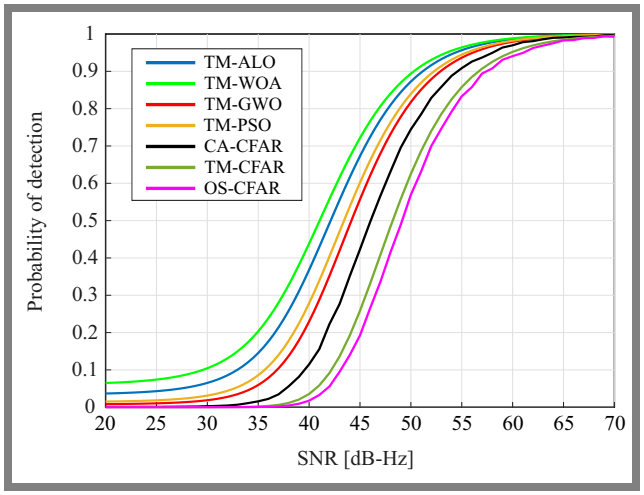

Fig. 5. Detection probability vs. SNR for three detectors: CA-CFAR, TM-CFAR and OS-CFAR, with and without optimization methods in a homogeneous environment.

a superior probability of detection when using the TM-CFAR detectors with optimization methods.

Tables 2–5 present the optimal values of the TM-CFAR parameters (T_d, T_p, k_{d1}, k_{d2}, k_{p1}, k_{p2}) in different scenarios. It has been observed that the best results are obtained when the parameters are identical (identical case). As a result, T_p and T_d are replaced by T and k_{d1}, k_{d2}, k_{p1}, k_{p2}, which take identical values k_1, k_2, for AND and OR fusion rules. Regarding the GNSS acquisition system, it is observed that the best results are obtained with a system that has the larger value of M. A degradation in detection performance is observed as the target false alarm probability decreases.

Furthermore, the influence of the AND and OR fusion rules is examined. It is evident that the best detection performance was achieved by a system utilizing the WOA and ALO algorithms followed by PSO and GWO for both OR and AND fusion rules. By comparing the results presented in Tabs. 2 and 3, a significant improvement in the probability of detection P_D

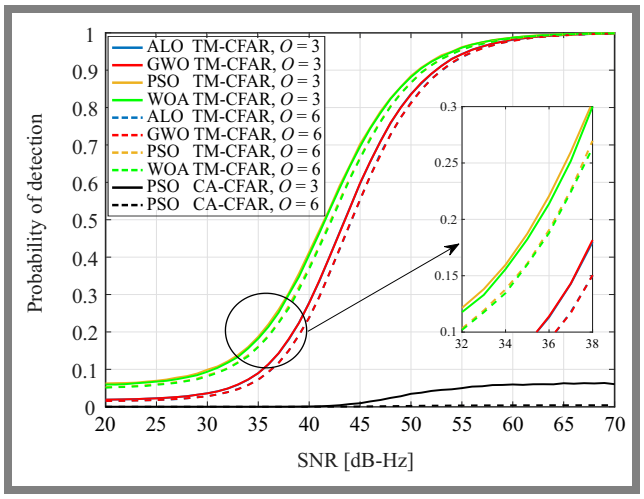

Fig. 6. Detection probability versus SNR for the TM-CFAR detector with optimization methods and the CA-CFAR detector.

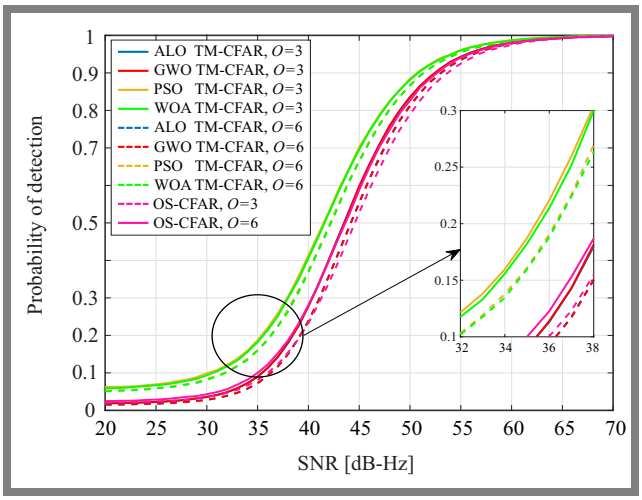

Fig. 7. Detection probability versus SNR for TM-CFAR and OS-CFAR detectors, with and without optimization methods.

is observed with the OR fusion rule, indicating that this rule offers better detection performance compared to the AND fusion rule.

Figure 5 presents the detection probability of TM-CFAR, CA-CFAR, and OS-CFAR detectors with and without optimization methods, when the number of reference cells is $M = 32$. CA-CFAR and OS-CFAR detectors are evaluated relative to the TM-CFAR detector under homogeneous conditions when optimization methods are employed. It is evident that CA-CFAR performs better than TM-CFAR in this environment. Moreover, the CA-CFAR algorithm outperforms both the TM-CFAR algorithm without optimization and the OS-CFAR algorithm.

Figure 6 compares CA-CFAR and TM-CFAR detectors in non-homogeneous environments with optimization techniques. It has been shown that the TM-CFAR algorithm surpasses its CA-CFAR counterpart in these environments. It should be noted that the problem addressed in this study focuses on the use of the TM-CFAR algorithm in non-homogeneous environments.

Figure 7 compares the TM-CFAR and OS-CFAR detectors with and without optimization techniques. It is demonstrated that the TM-CFAR algorithm surpasses the OS-CFAR algorithm.

Figure 8 shows the evolution of the total probability of detection P_D as a function of the variation in SNR for the AND fusion rule, using different optimization techniques, with a fixed number of reference cells $M = 32$, and in a situation in which the system contains two identical detectors. Based on this figure, it can be observed that the PSO technique provides the best performance compared to the remaining approaches.

Figure 9 illustrates the evolution of the overall probability of detection as a function of SNR, for the four cases: identical, non-identical, symmetrical and non-symmetrical. From this figure, we observe that the performance is better in the identical and symmetrical cases compared to the remaining scenarios.

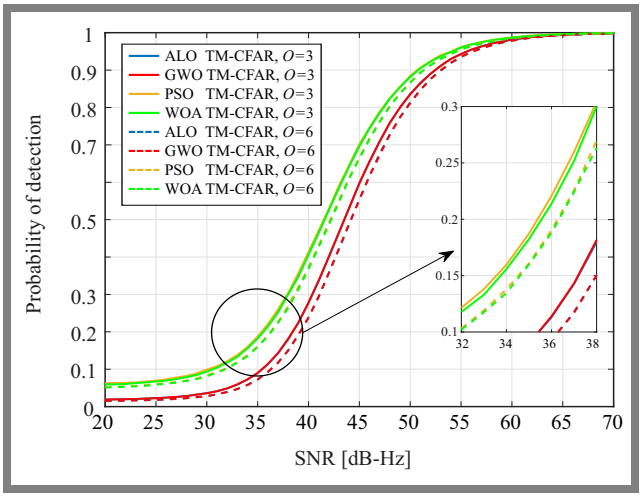

Fig. 8. Comparison between the four optimization algorithms of the TM-CFAR detector.

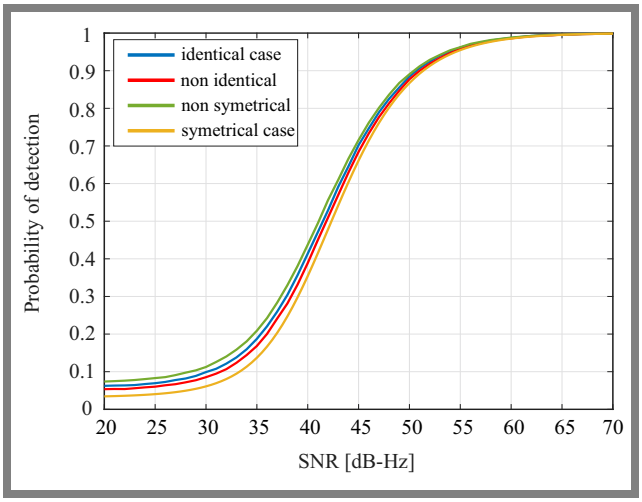

Fig. 9. Comparison of detection probability against SNR of the TM-CFAR detector for the four cases: identical, non-identical, symmetrical, and non-symmetrical, $P_{FA} = 10^{-4}$ and $M = 32$.

The evolution of the overall detection probability as a function of SNR variation is represented for the AND fusion rule

Tab. 4. Parameters estimated using the four optimization algorithms based on the number of cells with the OR fusion rule.

Number of cells	PSO	GWO	ALO	WOA
$M = 8$	$T = 3.5268$	$T = 2.7131$	$T = 3.5020$	$T = 3.5383$
	$k_1 = 1$	$k_1 = 1$	$k_1 = 1$	$k_1 = 1$
	$k_2 = 1$	$k_2 = 1$	$k_2 = 1$	$k_2 = 1$
	$P_D = 0.9987$	$P_D = 0.9986$	$P_D = 0.9988$	$P_D = 0.9987$
$M = 16$	$T = 1.5979$	$T = 3.6054$	$T = 3.6323$	$T = 5$
	$k_1 = 4$	$k_1 = 6$	$k_1 = 6$	$k_1 = 3.5563$
	$k_2 = 3$	$k_2 = 5$	$k_2 = 5$	$k_2 = 6$
	$P_D = 0.9994$	$P_D = 0.9992$	$P_D = 0.9992$	$P_D = 0.9992$
$M = 32$	$T = 0.5963$	$T = 1.5117$	$T = 0.9092$	$T = 0.8072$
	$k_1 = 6$	$k_1 = 7$	$k_1 = 6$	$k_1 = 6$
	$k_2 = 8$	$k_2 = 13$	$k_2 = 8$	$k_2 = 8$
	$P_D = 0.9998$	$P_D = 0.9996$	$P_D = 0.9995$	$P_D = 0.9996$

Tab. 5. Parameters estimated using the four optimization algorithms based on P_{FA} with the OR fusion rule.

Probability of false alarm	PSO	GWO	ALO	WOA
$P_{FA} = 10^{-4}$	$T = 0.5963$	$T = 1.5117$	$T = 0.9092$	$T = 0.8072$
	$k_1 = 6$	$k_1 = 7$	$k_1 = 6$	$k_1 = 6$
	$k_2 = 8$	$k_2 = 13$	$k_2 = 8$	$k_2 = 8$
	$P_D = 0.9998$	$P_D = 0.9996$	$P_D = 0.9995$	$P_D = 0.996$
$P_{FA} = 10^{-6}$	$T = 4.1283$	$T = 1.5834$	$T = 1.0286$	$T = 0.6289$
	$k_1 = 10$	$k_1 = 2$	$k_1 = 7$	$k_1 = 4$
	$k_2 = 13$	$k_2 = 10$	$k_2 = 4$	$k_2 = 6$
	$P_D = 0.9995$	$P_D = 0.9989$	$P_D = 0.9985$	$P_D = 0.9994$
$P_{FA} = 10^{-8}$	$T = 3.9342$	$T = 1.5500$	$T = 0.6495$	$T = 1.5285$
	$k_1 = 2$	$k_1 = 10$	$k_1 = 9$	$k_1 = 10$
	$k_2 = 12$	$k_2 = 6$	$k_2 = 1$	$k_2 = 6$
	$P_D = 0.9959$	$P_D = 0.9981$	$P_D = 0.9989$	$P_D = 0.9982$

in Fig. 10, for different values of P_{FA}, and a fixed value of the number of reference cells $M = 32$, in a system with two identical detectors. It can be seen from this figure that a decrease in false alarm probability P_{FA}, results in a significant degradation of detection probability.

Figure 11 shows the evolution of the probability of detection with respect to SNR for the AND fusion rules. It is shown that the higher the number of reference cells, the better the system and its detection performance.

To see the difference between the results obtained with the two fusion rules, i.e. AND and OR, more clearly, the variation in the total detection probability as a function of SNR for the two TM-CFAR detectors is presented.

The performance of the proposed system in terms of detection probability is shown in Fig. 12. It is evident from that figure that the system using the OR fusion rule outperforms the one employing the AND fusion rule in terms of detection probability.

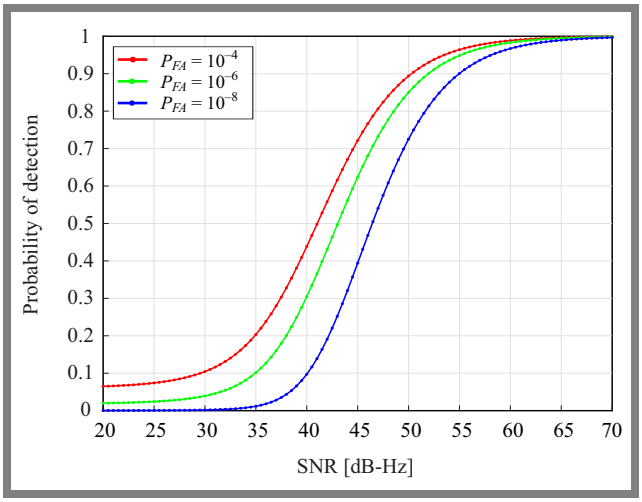

Fig. 10. Detection probability versus SNR of the TM-CFAR detector with different values of P_{FA}, in the case of $M = 32$.

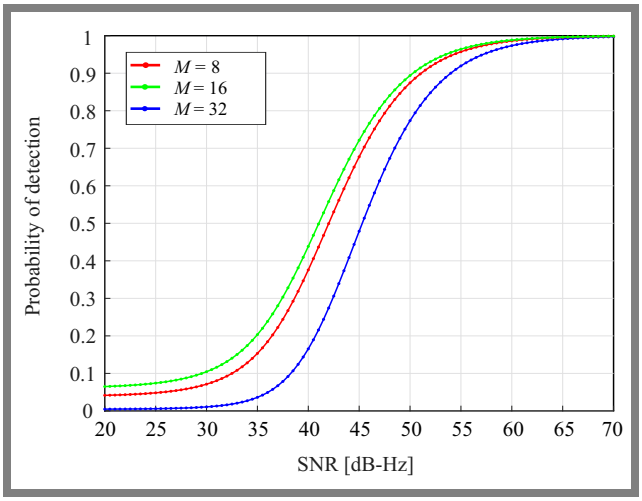

Fig. 11. Detection probability versus SNR of the TM-CFAR detector with different values of M, in the case of $P_{FA} = 10^{-4}$.

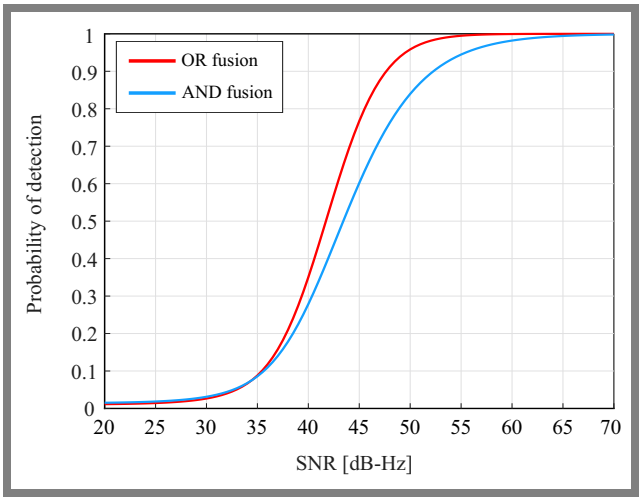

Fig. 12. Detection probability versus SNR of the TM-CFAR detector using PSO technique for AND and OR fusion rules in a scenario when $M = 32$ and with different detectors employed.

6. Conclusions

In this work, an attempt to enhance the efficiency of an approach based on metaheuristic optimization algorithms is presented to optimize the detection thresholds of TM-CFAR detectors. In this context, various simulations were performed, and the obtained results were compared and analyzed for different cases under consideration. The results indicate that applying these optimization methods enhances the performance of TM-CFAR detectors in non-homogeneous environments by enabling better estimation of scaling factors and estimated levels of noise power. Performance of the acquisition system is strongly influenced by the choice of fusion rules, as well as the use of identical or distinct detectors for the data and pilot channels.

The comparison of all optimization techniques revealed that PSO achieved the best performance in non-homogeneous environments. Furthermore, the OR fusion rule outperformed its AND counterpart, confirming the effectiveness of the proposed methods.

Acknowledgments

The presented work has been funded under the PRFU research project (no. A25N01UN300120220001) of the Algerian Ministry of Higher Education and Scientific Research (MESRS).

References

[1] K. Benachenhou, M. Hamadouche, and A. Taleb-Ahmed, "New Formulation of GNSS Acquisition with CFAR Detection", *International Journal of Satellite Communications and Networking*, vol. 35, pp. 215–230, 2017 (https://doi.org/10.1002/sat.1177).

[2] S. Dehouche and M. Hamadouche, "Enhanced Collective Detection for GNSS Weak Signals Acquisition in Rayleigh Channel", *International Journal of Satellite Communications and Networking*, vol. 36, pp. 332–351, 2018 (https://doi.org/10.1002/sat.1236).

[3] R. Grapenthin, "The Global Navigation Satellite System (GNSS): Positioning, Velocities, and Reflections", in: *Remote Sensing for Characterization of Geohazards and Natural Resources*, Springer, pp. 13–52, 2024 (https://doi.org/10.1007/978-3-031-59306-2_2).

[4] M.F. Hassani, A. Toumi, S. Benkrinah, and S. Sbaa, "Thresholding Optimization of Global Navigation Satellite System Acquisition with Constant False Alarm Rate Detection using Metaheuristic Techniques", *International Journal of Communication Systems*, vol. 37, art. no. 5938, 2024 (https://doi.org/10.1002/dac.5938).

[5] D. Ivković, A. Milenko, and Z. Bojan, "Detection of Very Close Targets by Fusion CFAR Detectors", *Scientific Technical Review*, vol. 66, pp. 50–57, 2016 (https://doi.org/10.5937/STR1603050I).

[6] K. Benachenhou, A. Taleb-Ahmed, and M. Hamadouche, "Performances Evaluation of GNSS ALTBOC Acquisition with CFAR Detection in Rayleigh Fading Channel", *IEEE Saudi International Electronics, Communications and Photonics Conference*, Riyadh, Saudi Arabia, 2013 (https://doi.org/10.1109/SIECPC.2013.6550786).

[7] D.U. Hai-Ming, M.A. Hong, and D.U. Bao-Qiang, "Adaptive TM-CFAR Detection Based on the Statistics ODV", *Journal of Beijing University of Posts and Telecommunications*, vol. 36, pp. 64–69, 2013 (https://journal.bupt.edu.cn/EN/Y2013/V36/I2/64).

[8] E.H. Houssein, A.G. Gad, K. Hussain, and P.N. Suganthan, "Major Advances in Particle Swarm Optimization: Theory, Analysis, and Application", *Swarm and Evolutionary Computation*, vol. 63, art. no. 100868, 2021 (https://doi.org/10.1016/j.swevo.2021.100868).

[9] J. Kennedy and E. Russell, "Particle Swarm Optimization", *IEEE International Conference on Neural Networks (ICNN'95)*, Perth, Australia, 1995 (https://doi.org/10.1109/ICNN.1995.488968).

[10] T.M. Shami *et al.*, "Particle Swarm Optimization: A Comprehensive Survey", *IEEE Access*, vol. 10, pp. 10031–10061, 2022 (https://doi.org/10.1109/ACCESS.2022.3142859).

[11] A. Sasithradevi, B. Chanthini, and S. Shoba, "A HybridOpt Approach for Early Alzheimer's Disease Diagnostics with Ant Lion Optimizer (ALO)", *Alexandria Engineering Journal*, vol. 109, pp. 112–125, 2024 (https://doi.org/10.1016/j.aej.2024.08.089).

[12] M.H. Nadimi-Shahraki, H. Zamani, Z.A. Varzaneh, and S. Mirjalili, "A Systematic Review of the Whale Optimization Algorithm: Theoretical Foundation, Improvements, and Hybridizations", *Archives of Computational Methods in Engineering*, vol. 30, pp. 4113–4159, 2023 (https://doi.org/10.1007/s11831-023-09928-7).

[13] L. Abualigah *et al.*, "Whale Optimization Algorithm: Analysis and Full Survey", in: *Metaheuristic Optimization Algorithms*, Morgan Kaufmann, pp. 105–115, 2024 (https://doi.org/10.1016/B978-0-443-13925-3.00015-7).

Elbahdja Ourfella, Ph.D. Student
LAGE laboratory
https://orcid.org/0009-0008-7843-4200
E-mail: ourfella.elbahdj@univ-ouargla.dz
Kasdi Merbah University, Ouargla, Algeria
https://www.univ-ouargla.dz

Sabra Benkrinah, Assoc. Prof.
LAGE laboratory
https://orcid.org/0000-0002-8292-2572
E-mail: benkrinah.sabra@univ-ouargla.dz
Kasdi Merbah University, Ouargla, Algeria
https://www.univ-ouargla.dz

Naceur Aounallah, Prof.
Department of Electronic and Telecommunications
https://orcid.org/0000-0001-9137-7900
E-mail: aounallah.naceur@univ-ouargla.dz
Kasdi Merbah University, Ouargla, Algeria
https://www.univ-ouargla.dz